Journal of Non-Crystalline Solids 356 (2010) 2683–2688

Contents lists available at ScienceDirect

Journal of Non-Crystalline Solids

journal homepage: www.elsevier.com/ locate/ jnoncrysol

Synthesis and characterization of glass–ceramic microspheres for thermotherapy

J.R. Martinelli [a,*], F.F. Sene [a], C.N. Kamikawachi [a], C.S. de M. Partiti [b], D.R. Cornejo [b]

[a] Nuclear and Energy Research Institute, Sao Paulo, Brazil
[b] Physics Institute, University of Sao Paulo, Brazil

ARTICLE INFO

Article history:
Received 6 October 2009
Received in revised form 6 April 2010
Available online 9 June 2010

Keywords:
Glass microspheres;
Mössbauer spectroscopy;
Hyperthermia;
Magnetic properties

ABSTRACT

Glass microspheres containing radionuclides are used to treat liver cancer. A promising alternative therapy is being developed based on the magnetic hyperthermia which is related to the heat supplied by a magnetic material under an alternating current magnetic field. The advantage of this option is that most of killed cells are cancer cells which are more susceptible to the temperature raise. In the present work aluminum iron silicate glasses containing minor glass modifiers and nucleating agents were synthesized as irregular shape particles which were further transformed in microspheres by using a petrol liquefied gas -oxygen torch. The optimized processing parameters which lead to microspheres that give a response to the magnetic field were determined. The dissolution rate in water at 90 °C was determined to be 3×10^{-8} g cm^{-2} min^{-1}. The microsphere size distribution was determined by laser scattering. The crystalline phase responsible for the ferromagnetic response was identified as magnetite. Since this phase has a high saturation magnetization and high Curie temperature, it is potentially useful for biomedical applications. The hysteresis magnetic loop was measured for materials produced in different conditions, and some of them showed to be appropriated for thermotherapy. The ratio Fe^{3+}/Fe_{total} was determined by Mössbauer spectroscopy.

1. Introduction

Hepatocellular Carcinoma (HCC) is one of most common forms of cancer worldwide. The majority of HCC patients are not surgical candidates, and do not qualify for liver transplant due to advanced stage of cancer at diagnosis. One among possible therapeutic options is the use of transarterial administration of Yttrium-90 containing glass microspheres [1–3]. In that case the microspheres are injected in the liver through a catheter introduced in the hepatic artery. This therapeutic method assumes that the liver tumors are hypervascular, so most of the microspheres migrate to lesioned region, and the microspheres are trapped in arterioles which feed the tumors. This therapeutic option then allows the treatment of unresectable HCC, surgical downstaging, and even makes possible transplantation. ^{90}Y has been selected as the major radionuclide because it is a pure beta-emitter, has an average beta emission energy of 0.9367 MeV, average penetration range in tissue is 2.5 mm, physical half-life is 64.2 h and decays to stable zirconium-90. Others radionuclides have also been proposed for that application, such as ^{32}P [4,5], and ^{166}Ho, both of them with their own advantages and drawbacks.

Several alternative techniques have been used to eliminate tumors by the use of heat. Use of hot water, exposition to infrared rays, use of ultrasound, and microwaves are the most common ones, nevertheless none were effective to heat locally and deeply tumors.

Hyperthermia seems to be an alternative way to annihilate cancer cells. Magnetic induction hyperthermia is a technique for destroying cancer cells when magnetic particles are introduced in the patient. When the material is exposed to external magnetic fields, the local temperature is raised in the range of 42 to 46 °C by indirect heating, and consequently, the cancer tissue is annihilated [6].

The advantages of this procedure are the absence of ionizing radiation, and the fact that most of exterminated cells are cancer cells which are more susceptible to the temperature raise. Aggressive cancer cells are softer than their healthy counterparts. The temperature boost may weaken the protein scaffolding within the cancer cell's nucleus, making the nuclear DNA more vulnerable to chemotherapy and radiation. Among the benefits of this therapy is: highly localized, predictable tumors volume, cancer cells perish around 43 °C, tumors are easier heated than normal tissues, few side effects, and hyperthermia can also enhance the effects of certain anticancer drugs.

A large number of magnetic materials for magnetic induction hyperthermia have been evaluated [7–12], including magnetic glass–ceramics [13–19].

For this specific application the material must contain a considerable amount of ferromagnetic phases which are responsible to generate and dissipate the heat. Another important requirement is the biocompatibility, low cytotoxicity level, and high chemical durability.

* Corresponding author.
E-mail address: jroberto@ipen.br (J.R. Martinelli).

0022-3093/$ – see front matter © 2010 Elsevier B.V. All rights reserved.
doi:10.1016/j.jnoncrysol.2010.05.006

Among the materials which could be used in hyperthermia are: ferromagnetic crystals, magnetite (Fe_3O_4), and maghemite (γ-Fe_2O_3).

Glass-ceramic materials based on CaO, P_2O_5, SiO_2 and Fe_2O_3 were previously investigated for this purpose [20]. It was shown that magnetite was nucleated after a heat treatment and it was the major crystalline phase embedded in the glass matrix but some hematite and maghemite were also present. The material presents a ferrimagnetic behavior.

Ferrimagnetic magnetite microspheres 20–30 μm in diameter were also prepared by melting powders in high-frequency induction thermal plasma, and by precipitation from an aqueous solution; the latter was considered a promising thermoseed for hyperthermic treatment of cancer. Nevertheless, the surface presents some roughness which could lead to traps in the bloodstream [21].

Downgrading the particle size distribution, spinel iron oxide nanoparticle/organic hybrid 7 to 23 nm was synthesized and the heat generation of such particles was evaluated under an ac magnetic field. These materials would be useful as a biocompatible material for hyperthermia [22].

Other developed materials are: LiFe5O8 in α-Fe_2O_3 matrix, magnetite in a matrix of β-wollastonite and calcium phosphorous borosilicate glassy phase, α-Fe, magnetite in a boron free phosphorous calcium silicate phase, and zinc–iron ferrite in a calcium silicate glassy phase.

The main goal of this study is to produce and evaluate ferromagnetic glass–ceramic microspheres suitable for liver cancer treatment. Comparing with previously reported materials, in the present work microspheres were produced from irregular shape particles based on aluminum iron silicate glasses by heating those particles using a Petrol Liquefied Gas/ oxygen torch. It is expected that the viscosity of the amorphous phase is reduced and the particles are shaped to microspheres maintaining the ferromagnetic phase, and a very good smooth surface, with no cutting edges and other flaws, so those particles should be able to flow easily through the bloodstream up to the liver. The particle size distribution must also be appropriated to avoid undesirable embolization of the hepatic artery before being undertaken by the liver, and be trapped in the vascular region surrounding the cancer tissue. The control of the iron concentration in the microspheres, the size distribution, and the iron valence state are directly related to the electromagnetic field absorption efficiency. The optimized processing parameters leading to microspheres which present some response to the alternating magnetic field were determined. Although the saturation of magnetization for magnetite is around 92 emu/g, it is expected to obtain materials with lower magnetization values due to the presence of other ferric phases (α-Fe_2O_3 and γ-Fe_2O_3), however, the temperature increase will be measure during the exposition to a magnetic field to evaluate the efficiency of the energy absorption by the material.

2. Experimental procedure

Glasses based on the compositions showed in Table 1 were prepared by mixing analytical grade SiO_2 , Al_2O_3, Fe_2O_3, TiO_2, CaO, Na_2CO_3 and MnO, melted in an electric furnace at 1550 °C for 2 h, and stirring each 30 min with a high purity silica rod to achieve a good homogeneity and fining. An alumina crucible was used for this purpose. After casting, the material was ground using a stainless steel pestle and mortar and sieved to separate particles in the size range of 38–63 μm. The final composition of the glass was determined by Energy Dispersive X-rays Analysis (EDX Shimadzu model 720).

The compositions proposed in Table 1 are based on the ability to form glasses according to the theory proposed by Zachariasen [23]. Since a ferromagnetic material is desired, these compositions contain iron with relatively high concentration as one of the component. Besides that, those glasses present chemical durability appropriated for the aimed application. Different compositions were investigated since no reported data concerning the properties optimization have been previously reported.

Table 2 presents an example of a glass composition (nominal and final composition).

Crushed glass particles with irregular shapes were transformed to microspheres by using a process reported elsewhere [24] known as “spheronization by flame”. A torch burning a mixture of oxygen (1–3 L/min) and Petrol Liquefied Gas (1–2 L/min) was used for this purpose. The microspheres were collected in a metal tube. The experimental parameters had to be adjusted to reach the best results.

The desired particle size distribution should be in the range of 20–40 μm because that is the suitable particle size to match the blood capillaries caliber in the liver tissue. So, particles in this size range should flow directly to the cancer tumor and being trapped.

Glass samples and microspheres were analyzed by X-rays Diffraction (XRD - Rigaku model Multiflex), and Scanning Electron Microscopy (SEM- Philips model XL-30).

The Mössbauer spectra were obtained at room temperature with a conventional constant-acceleration spectrometer in a 10 mC Rh ^{57}Co source. The absorber unit was prepared by pressing the powder sample (0.2 g) between two Lucite plates 1.5 cm in diameter added to materials that are transparent to the radiation. The velocity of the source was calibrated using a pure iron foil that was also used as a reference for the isomer shift. In this study, Mössbauer Spectroscopy is a technique of great interest because it differentiates the various oxidation states. It also presents advantages such as quantification of relative proportions of iron sites in a sample.

Zero field cooling (ZFC) and field cooling (FC) magnetization curves, as well as hysteresis loops were determined by using a vibrating sample magnetometer coupled to a superconducting coil with 90 kOe of maximum applied filed.

Samples $10 \times 10 \times 1$ mm^3 were immersed in water at 90 °C during 21 days to determine the dissolution rate. The sample's weight was monitored after 1, 3, 7, and 14 days. All measurements were replicate with three different samples and the results presented are an average of these data.

The particle size distribution was determined by the laser scattering technique (Cilas Model 1064).

To check the response of microspheres when exposed to ac current magnetic field, 0.1 g of microspheres were immersed in a glass

Table 1
Glass composition.

Component	Nominal composition range (wt.%)
SiO_2	20–40
Fe_2O_3	30–40
Al_2O_3	10–20
TiO_2	2–6
CaO	3–5
Na_2O	5–10
MnO	0.5

Table 2
Nominal and final glass composition for glass type 3.

Component	Nominal (wt.%)	Experimental (wt.%)
SiO_2	31.81	8.788
Fe_2O_3	44.72	56.099
Al_2O_3	8.63	22.187
TiO_2	4.24	5.323
CaO	3.09	3.372
Na_2O	6.97	3.446
MnO	0.55	0.551
Cr_2O_3	–	0.102
CuO	–	0.08
MoO_3	–	0.032
SrO	–	0.02

container with 3 mL of distilled water. An induction generator (Politron model I-25, 2 MHz, 2500 W) was used for that purpose. The container was surrounded by a copper coil 20 mm in diameter, and the current flowed for 5 min. The temperature inside the glass container was monitored by a mercury free glass thermometer with a good precision.

3. Results

The dissolution rate was determined to be 3×10^{-8} g/(cm^2 min) in the pH = 7.

Fig. 1a and b shows the SEM of irregular glass particles and the resulting microspheres, respectively.

Fig. 2a and b shows the particle size distribution of glass particles and the resulting microspheres.

Fig. 3 a–c shows the XRD patterns for as-prepared microspheres and after heat treatments at 650 °C in oxygen and Ar/H_2 atmosphere, respectively.

Fig. 4 a–c shows the Mössbauer spectra for microspheres with increasing amount of Fe in the glass composition.

Table 3 presents the Mössbauer hyperfine parameters and relative subspectral area.

Fig. 5 a–c shows the Zero field cooling and field cooling spectra for one series of microspheres.

Fig. 6 a–c shows the hysteresis curves for three distinguished samples related to the ZFC and FC curves presented above.

Table 4 presents the temperature difference (ΔT) measured during the microspheres exposition in ac current magnetic field.

4. Discussion

The presence of Al in the glass composition is high but its dissolution in the blood stream is very low, and the influence of this element on the biocompatibility is not relevant. These results have been previously reported [4].

Table 2 shows a significant variation in the amount of SiO_2 and Al_2O_3 when the final composition is compared to the nominal composition. This fact is attributed to the use of an alumina crucible which can be partially dissolved into the glass composition, and also favors the incorporation of some elements during the melting. However, even though the amount of SiO_2 decreases in comparison with the nominal value, a glass is still formed.

The dissolution rate of the material (3×10^{-8} g/(cm^2 min)) is compatible with a good chemical durability, comparing to the USDOE value (2×10^{-8} g/(cm^2 min)) for materials designed for the immobilization of nuclear wastes [25].

Fig. 1a displays the morphology of the crushed glass particles. It is noticeable in the figure a diversity of sizes and aspect ratios, some of them with relatively large values. The corresponding particle size distribution is displayed in Fig. 2a and presents an appearance like bimodal-type distribution where it is possible to see the presence of some large particles (even after sieving). Consequently, the corresponding microspheres have sizes that would be larger than the one previously expected (for example, Fig. 1a shows the existence of microspheres whose sizes surpass 100 μm in diameter). In Fig. 2b is showed the microspheres size distribution. It is clearly visible that this curve presents a monomodal shape and the maximum is displaced to

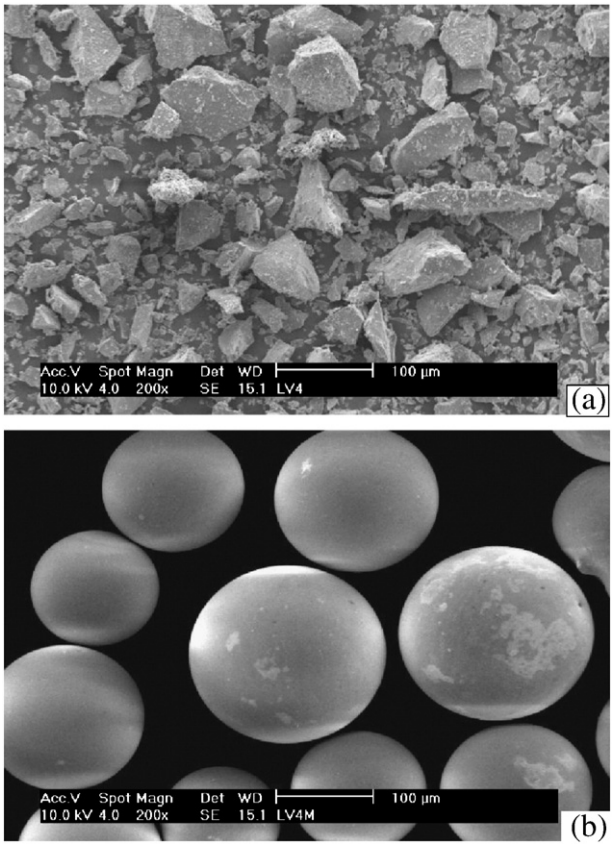

Fig. 1. (a) SEM of irregular glass particles and (b) the resulting microspheres.

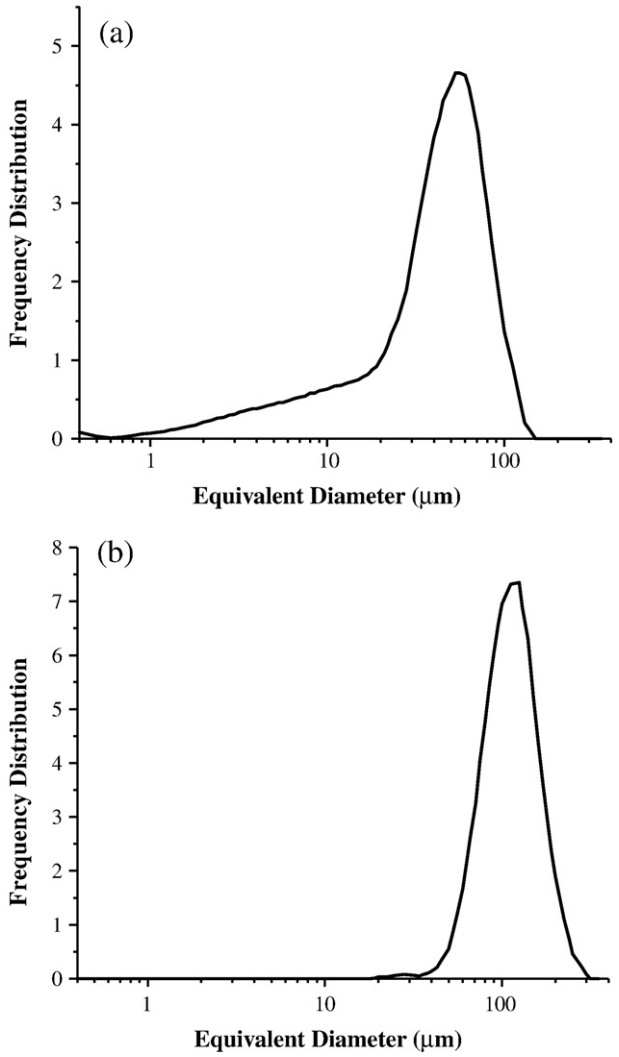

Fig. 2. (a) the particle size distribution of glass particles, and (b) the resulting microspheres.

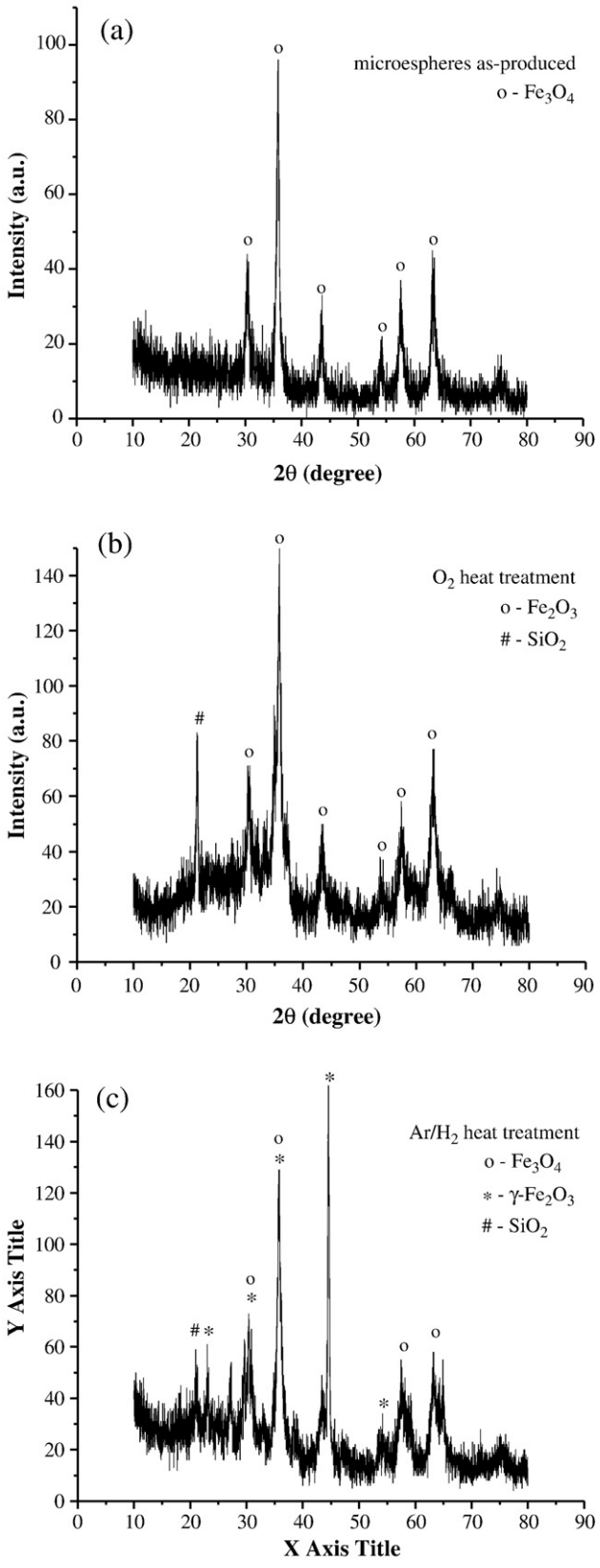

Fig. 3. XRD patterns for a) as-prepared microspheres and after a heat treatment at 650 °C in (b) oxygen, and (c) Ar/H_2 atmosphere.

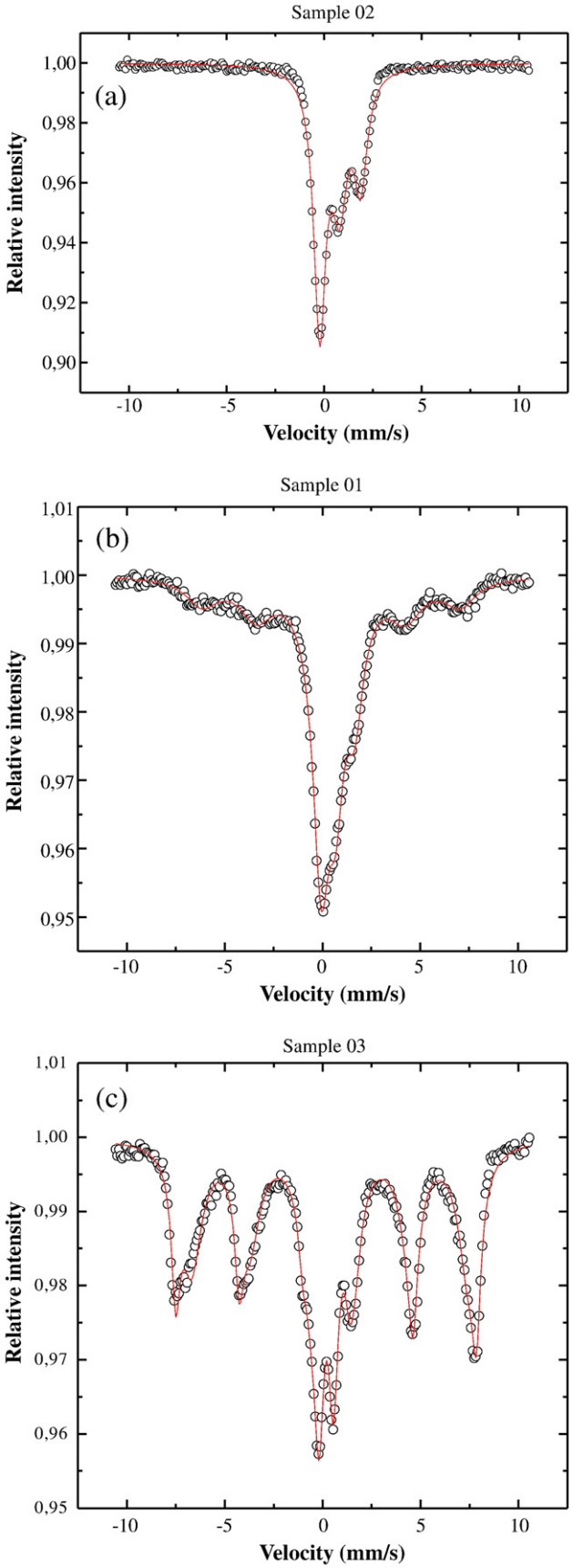

Fig. 4. a–c. the Mössbauer spectra for microspheres with increasing amount of Fe in the glass composition.

higher values, in comparison with the original size distribution of irregular particles.

According to X-ray diffraction pattern showed in Fig. 3a the as-produced microspheres have only Fe_3O_4 crystalline phase. By heat

Table 3
Mössbauer hyperfine parameters and relative subspectral area.

Sample	Δ1 (mm/s)	IS1(mm/s)	AR1(%)	Δ2 (mm/s)	IS2(mm/s)	AR2(%)
2	2.14(1)	0.94(1)	46	0.98(1)	0.44(1)	54

Samples	Δ1 (mm/s)	IS1 (mm/s)	AR1(%)	Δ2 (mm/s)	IS2 (mm/s)	AR2(%)	Bhf3(T)	IS3 (mm/s)	AR3(%)	Bhf4(T)	IS4 (mm/s)	AR4(%)
1	1.68(6)	0.96(4)	27	0.77(5)	0.43(2)	39	41(2)	0.57(3)	34			
3	2.12(3)	0,68(1)	10	0.72(1)	0.32(1)	19	43.8(1)	0.50(1)	49	47.5(1)	0.31(1)	22

1- Fe^{2+} doublet Δ — quadrupole splitting 2- Fe^{3+} doublet IS — Isomer shift.
Bhf-Hyperfine field AR — relative subspectral area.

treating the microspheres at 650 °C in an oxidizing atmosphere, only Fe_3O_4 and a strong peak of SiO_2 is noticed (Fig. 3b). If the thermal treatment is performed at 650 °C but in reducing atmosphere, Fe_3O_4 and γ-Fe_2O_3 phases are now evidenced (a small peak due to the crystallization of SiO_2 is also observed), as displayed in Fig. 3c. The increase of the relative amount of Fe^{2+} in the sample composition could explain the crystallization of γ-Fe_2O_3 during the subsequent heat treatment in an oxidizing atmosphere.

The crystallite size of Fe_3O_4 was estimated from the Scherrer's equation considering the peak at $2\theta = 35.86$ degrees in the X-rays diffraction patterns. For the as-produced microspheres (Fig. 3 (a)) the crystallite size is 16 nm. For the microspheres submitted to heat treatments in oxidizing and reducing atmospheres (Fig. 3 (b) and (c)), the crystallite size was determined to be 10 nm in both cases.

Concerning the Mössbauer spectroscopy, it can be noticed that for glasses with lower iron content only doublet of Fe^{2+} and Fe^{3+} are observed (sample 2 in Fig. 4a). When the amount of iron is increased in the glass composition, sextets related to arranged magnetic phases are observed (Fig. 4b and c). According to Table 3 the amount of Fe^{3+} also increases and the ratio Fe^{3+}/Fe^{2+} changes from 1.7 to 9.0

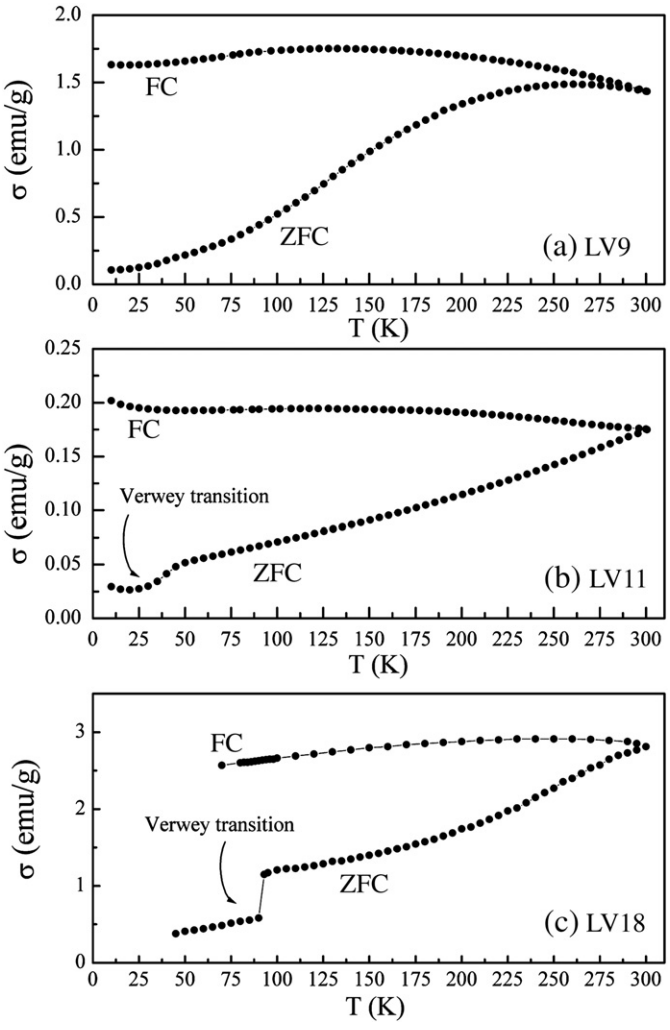

Fig. 5. a–c. the Zero field cooling and field cooling spectra for one series of microspheres.

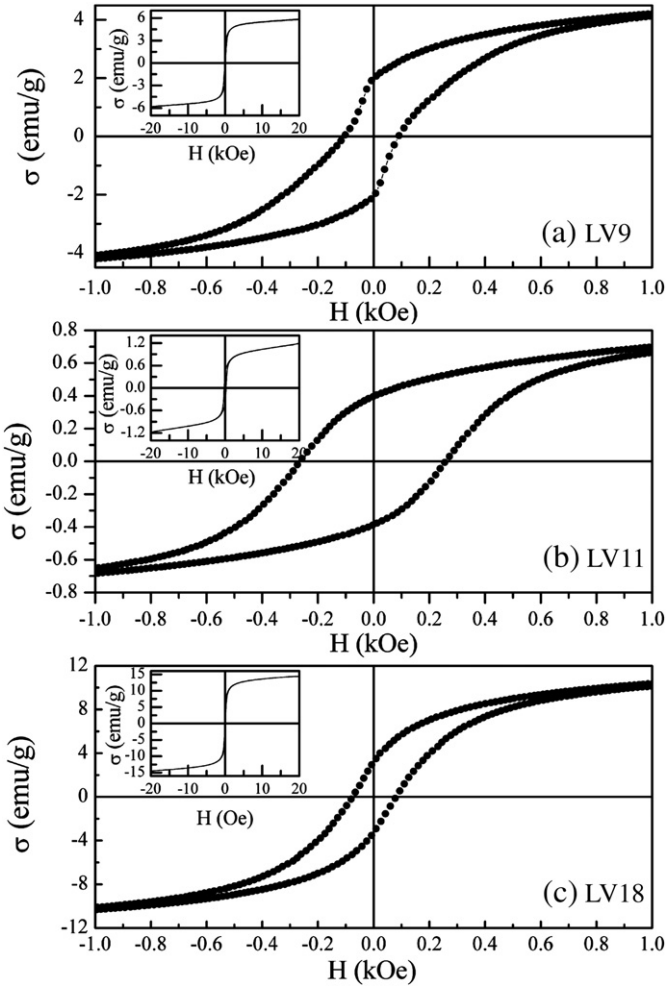

Fig. 6. a–c. the hysteresis curves for three distinguished samples.

Table 4
Temperature difference measured during the microspheres exposition in ac current magnetic field.

Glass type	ΔT (°C)
LV09 (sample 2)	10 ± 2
LV11 (sample 1)	13 ± 2
LV14	11 ± 2
LV15	13 ± 2
LV16	11 ± 2
LV18 (sample 3)	32 ± 2

$\Delta T = Tmax - T_{R.T.}$ where T max is the maximum temperature measured after 5 min and $T_{R.T.}$ is the room temperature.

following the variation of the relative subspectral area. The analysis of the Mössbauer spectrum shows the presence of an arranged magnetic phase with hyperfine field that could be associated to magnetite. The quantity of this phase was estimated to be 34% in sample 1 and even higher (49%) in sample 3.

Fig. 5 shows the ZFC and FC magnetization curves for samples with increasing iron content and Fig. 6 the corresponding hysteresis loops at room temperature. For the sample with less iron content (named LV9) the ZFC-FC curve (Fig. 5a) shows a blocking temperature close to room temperature (290 K, where ZFC reached a maximum value). So, it can be assumed that the crystallite size of magnetite in this sample is significantly small and a considerable fraction of the Fe_3O_4 is in the superparamagnetic regime at room temperature. In fact, a relatively small grain size can prevent the observation of the Verwey transition [26], which was not seen in this sample. The corresponding hysteresis loop (Fig. 6a) with a convex second-quadrant is compatible with this picture. Therefore, this sample should present a superparamagnetic behavior at room temperature and would not be suitable for hyperthermia. Fig. 5b, on the other hand, does not exhibit a blocking temperature up to 300 K, so that the sample named LV11 is ferromagnetic at room temperature. The Verwey transition is observed around 40 K which is compatible with "nanosized" crystallites of magnetite [26]. In this case, the hysteresis loop (Fig. 6b) shows a second-quadrant concave and a coercive field relatively high (280 Oe). However, the high SiO_2 content produces a poor magnetization in the sample (only 1.2 emu/g at the saturation). Finally, in the case of sample named LV18 (Fig. 5c) no blocking temperature up to room temperature is observed, and the Verwey transition is clearly visible at 90 K (much closer to the 124 K expected for bulk magnetite), indicating an increase in the crystallite size for this sample. The hysteresis cycle (Fig. 6c) displayed a reasonable coercive field (100 Oe) and a saturation magnetization close to 15 emu/g, i.e. much higher than the sample LV11. Then, this material seems to be potentially useful for hyperthermic applications.

The heating test performed by exposing the material to an external alternating field showed that samples with higher amount of iron present the highest temperature difference (see Table 4). This fact is related to the higher amount of magnetite in the glass matrix. The best material (sample LV18) has a composition with the higher ratio of iron oxide/aluminum oxide which can provide the formation of a stable magnetite phase during the process to obtain microspheres.

According to previously published data [22], the saturation magnetization for ferromagnetic nanospheres (8–14 nm) is approximately 78 emu/g. If those materials are exposed to alternate magnetic fields (230 kHz} with field intensity around 100 Oe, the absorbed energy causes a temperature increase from room temperature to approximately 38–44 °C. However, those materials are not adequate for the present application due to the relatively small particle size. Nanoparticles are not trapped in the blood capillaries that feed the tumors in the liver and they would be distributed throughout the liver, not taken the advantage of the hypervascularity characteristic of the region surrounding the tumor. Silica microspheres (20–30 μm) containing magnetite were also produced and present a saturation magnetization in the range of 32–92 emu/g, and coercive fields of 50–120 Oe [10]. Although those materials are suitable for energy absorption and consequently heat generation, their surfaces seem to present some flaws which would be unfavorable for the present application. Besides that, no chemical durability data have been reported. In the present work glass–ceramic microspheres were produced with lower saturation magnetization; however they have smooth surfaces which are ideal to be introduced into the hepatic artery, without being trapped on the way to the liver. Although the saturation magnetization for these materials are lower compared to the ones previously reported [10,22], by exposing them to an alternate magnetic field (2 MHz, 2500 W), a substantial increasing in the temperature was observed, even for the unfavorable field (alternate magnetic fields with frequency around 450 kHz are more adequate for this purpose). The magnetization is related to the magnetite content, and it is expected that the amount of magnetite can be increased after performing an appropriated heat treatment in oxygen, but always restricting the temperature range to prevent shape deformation in the microspheres.

5. Conclusions

In this work, chemical resistant glass microspheres with potential use in hypertermic therapy were produced. The major crystalline phase present was magnetite. Glasses containing the highest iron content shown Mössbauer spectra with doublets related to the ions Fe^{2+} and Fe^{3+} as well as sextets related to the ordered magnetic phases. The amount of Fe^{3+} increases and the ratio Fe^{3+}/Fe^{2+} changes from 1.7 to 9.0 following the variation of the relative subspectral area. For a particular glass composition there is no blocking temperature up to 300 K in the ZFC and FC curves, and a Verwey transition around 90 K. This material presents magnetic saturation close to 15 emu/g and coercive field of 100 Oe. Previously reported data for other materials containing magnetite showed improved saturation magnetization and consequently better heat generation under ac external magnetic field compared with the present data. However, those materials are not adequate for the aimed application. The heating test of the material developed in the present work when exposed to ac magnetic field shows that this material absorbs energy and generates heat, and could become a potentially material for applications in hyperthermia if the saturation magnetization is increased.

Acknowledgement

The authors acknowledge CNPq (Universal 475212/2007-0, 501005/2008-0), and Fapesp (05/53241-9) for the financial support.

References

[1] G.J. Ehrhardt, D.E. Day, Nucl. Med. Biol. 14 (1987) 233.
[2] M.J. Hyatt, D.E. Day, J. Am. Ceram. Soc. 70 (1987) 283.
[3] E.M. Erbe, D.E. Day, J. Biomed. Mater. Res. 27 (1993) 1301.
[4] F.F. Sene, J.R. Martinelli, E. Okuno, J. Non-Cryst. Solids 354 (2008) 4887–4893.
[5] L. Liu, Z. Jiang, G.-J. Teng, J.-Z. Song, D.-S. Zhang, Q.-M. Guo, W. Fang, S.-C. He, J.-H. Guo, World J. Gastroenterol. 5 (6) (1999) 492.
[6] O. Bretcanu, E. Verne´, M. Coisson, P. Tiberto, P. Allia, J. Magn and Magn. Mater. 305 (2006) 529.
[7] A. Jordan, R. Scholz, P. Wust, H. Fahling, R. Felix, J. Magn. Magn. Mater. 201 (1999) 413.
[8] S.A. Gómmez-Lopera, R.C. Plaza, A.V. Delgado, J. Colloid Interf. Sci. 240 (2001) 40.
[9] K. Takegami, T. Sano, H. Wakabayashi, J. Sonoda, T. Yamazaki, S. Morita, T. Shibuya, A. Uchida, J. Biomed. Mater. Res. (1998) 210.
[10] M. Kawashita, M. Tanaka, T. Kokubo, Y. Inoue, T. Yao, S. Hamada, T. Shinjo, Biomaterials 26 (2005) 2231.
[11] J.H. Park, K.H. Im, S.H. Lee, D.H. Kim, D.Y. Lee, Y.K. Lee, K.M. Kim, K.N. Kim, J. Magn. Magn. Mater. 293 (2005) 328.
[12] M.H. Araujo Guedes, et al., J. Magn. Magn. Mater. 293 (2005) 283.
[13] H. Matsuki, T. Satoh, K. Murakami, T. Hoshino, T. Yanada, S. Kikuchi, IEEE Trans. Magn. 26 (1990) 1551.
[14] T. Kokubo, T. Yamamuro, Y. Ebisawa, K. Ohura, European Patent 361797, 1990.
[15] Y. Ebisawa, F. Miyaji, T. Kokubo, K. Ohura, T. Nakamura, Bioactivity of ferromagnetic glass ceramics in the system FeO–Fe2O3–CaO–SiO2, Biomaterials 18 (1997) 1277–1284.
[16] H. Konaka, F. Miyaji, T. Kokubo, J. Ceram. Soc. Japan 105 (1997) 833.
[17] S.H. Oh, S.Y. Choi, Y.K. Lee, K.N. Kim, J. Biomed. Mater. Res. 54 (2001) 360.
[18] D. Arcos, R.P. del Real, M. Vallet-Regi, Biomaterials 23 (2002) 2151.
[19] R.K. Singha, G.P. Kothiyalb, A. Srinivasan, Magn. Magn. Mater 320 (2008) 1352.
[20] D. Eniu, et al., J. Mag. and Mag. Mater. 293 (2005) 310.
[21] M. Kawashita, et al., Biomaterials 26 (2005) 2231.
[22] K. Hayashi, et al., J. Mater. Res. 23 (2008) 3415.
[23] W.H. Zachariasen, J. Am. Soc. 54 (1938) (1938) 3841.
[24] W. Huang, et al., The Preparation and application of the micro-spheres containing Yttrium-90, J. Shanghai Inst. of Bldg. Mat. 4 (1992) 347.
[25] W. Huang, D.E. Day, C.S. Ray, C.W. Kim, S.T.D. Reis, Glass Sci. Technol. 77 (2004) 1.
[26] G.F. Goya, T.S. Berquo, F.C. Fonseca, M.P. Morales, J. Appl. Phys. 94 (2003) 3520.